

# StrassenNets: Deep learning with a multiplication budget

Michael Tschannen<sup>\*1,2</sup>, Aran Khanna<sup>†2</sup>, and Anima Anandkumar<sup>‡2,3</sup>

<sup>1</sup>ETH Zürich      <sup>2</sup>Amazon AI      <sup>3</sup>Caltech

October 31, 2022

## Abstract

A large fraction of the arithmetic operations required to evaluate deep neural networks (DNNs) are due to matrix multiplications, both in convolutional and fully connected layers. Matrix multiplications can be cast as 2-layer sum-product networks (SPNs) (arithmetic circuits), disentangling multiplications and additions. We leverage this observation for end-to-end learning of low-cost (in terms of multiplications) approximations of linear operations in DNN layers. Specifically, we propose to replace matrix multiplication operations by SPNs, with widths corresponding to the budget of multiplications we want to allocate to each layer, and learning the edges of the SPNs from data. Experiments on CIFAR-10 and ImageNet show that this method applied to ResNet yields significantly higher accuracy than existing methods for a given multiplication budget, or leads to the same or higher accuracy compared to existing methods while using significantly fewer multiplications. Furthermore, our approach allows fine-grained control of the tradeoff between arithmetic complexity and accuracy of DNN models. Finally, we demonstrate that the proposed framework is able to rediscover Strassen’s matrix multiplication algorithm, i.e., it can learn to multiply  $2 \times 2$  matrices using only 7 multiplications instead of 8.

## 1 Introduction

The outstanding predictive performance of deep neural networks (DNNs) often comes at the cost of large model size, and corresponding computational inefficiency, hindering their deployment on mobile and embedded hardware. For example, a full precision ResNet-152 contains 60.2 million parameters and one forward pass requires 11.3 billion floating point operations (FLOPs). A variety of methods to address this issue were proposed recently, including architectural optimizations [1, 2, 3, 4], factorization of weight tensors [5, 6, 7, 8, 9, 10], pruning of weights [11, 12, 13, 14], and reducing the numerical precision of weights and activations [15, 16, 17, 18, 19] (see Section 2 for a more detailed overview).

In this paper, we choose *reducing the number of multiplications* as our guiding algorithm design principle. This design principle has led to many fast algorithms in the past, most notably Strassen’s matrix multiplication algorithm [20], which uses 7 instead 8 multiplications to compute the product of two  $2 \times 2$  matrices (and requires  $O(n^{2.807})$  operations for multiplying  $n \times n$  matrices). In the context of deep neural networks (DNNs), the same design principle led to the Winograd filter-based convolution algorithm proposed by [21], which only requires 16

---

<sup>\*</sup>michaelt@nari.ee.ethz.ch

<sup>†</sup>arankhan@amazon.com

<sup>‡</sup>anima@amazon.com

Work done while all authors were at Amazon.

instead of 36 multiplications to compute  $2 \times 2$  outputs of 2D convolutions with  $3 \times 3$  kernels. This strategy achieves a  $2\text{--}3\times$  speedup on GPU in practice. From a hardware implementation (ASIC) perspective, reducing the number of multiplications is beneficial as multiplication operations consume significantly more energy than addition operations [22, 23]. Furthermore, encoding an addition/subtraction as binary  $\{-1, 1\}$  weight is much more storage efficient, and hence more energy efficient on ASIC [24], than encoding a multiplication with an 8bit integer or a 32bit floating point weight. Moreover, it was demonstrated recently that DNN architectures which rely on a large number of additions and a small number of multiplications (such as [18]) achieve a 60% higher throughput on FPGA than on GPU, while being  $2.3\times$  better in performance/watt [25].

Here, we take the design principle of reducing the number of multiplications one step further and propose a novel framework to drastically reduce the number of multiplications used by DNNs for inference. Specifically, for every DNN layer, we cast the (matrix) multiplication of the weight matrices with the activations as a 2-layer sum-product network (SPN) (arithmetic circuit) that disentangles (scalar) multiplications and additions in a way similar to Strassen’s algorithm. The number of hidden units in the SPNs thereby determines the multiplication budget of the corresponding DNN layers. However, unlike Strassen’s algorithm or Winograd filter-based convolution, which rely on hand-engineered transforms (that can be expressed as SPNs as well), we *learn the addition and multiplication operations for all layers jointly from data* by learning the edges of the SPNs, encoded as ternary  $\{-1, 0, 1\}$  matrices, for each layer. This allows us to reduce the number of multiplications much more drastically than Strassen’s algorithm or Winograd filter-based convolution as our transforms are approximate and adapted to the weight matrices and distributions of the activations/features in the DNN at hand. In more detail, our contributions are the following.

- We propose a SPN-based framework for stochastic gradient-based end-to-end learning of fast approximate transforms for the arithmetic operations in DNN layers.
- Our framework allows fine-grained control of the number of multiplications and additions used at inference time, thereby enabling precise adjustment of the tradeoff between arithmetic complexity and accuracy of DNN models.
- Extensive evaluations on CIFAR-10 and ImageNet show that our method applied to ResNet yields significantly higher accuracy than existing methods for a given multiplication budget, or leads to the same or higher accuracy compared to existing methods while using significantly fewer multiplications. For ResNet-18 our method reduces the number of multiplications by 99.3% compared to the full-precision model while incurring a top-5 accuracy decrease of only 1.9%.
- We demonstrate that the proposed framework is able to rediscover Strassen’s algorithm, i.e., it can learn to multiply  $2 \times 2$  matrices using only 7 multiplications instead of 8.

We continue by reviewing related work in Section 2 and then describe our framework and its application to 2D convolution in Section 3. A detailed numerical evaluation of our framework is presented in Section 4 and concluding remarks can be found in Section 5.

## 2 Related work

We briefly review the most common approaches to make DNNs more compute efficient. In all cases, there is a tradeoff between the complexity reduction and reduction in the (inference) accuracy of the model being compressed.

A popular way to speed up DNNs, in particular convolutional neural networks (CNNs), is to conceive architectures and layers in a resource-efficient manner. Examples of such architectures are SqueezeNet [1], MobileNet [2], and ShuffleNet [3]. SqueezeNet reduces the convolution kernel size, whereas MobileNet and ShuffleNet rely on depth-wise separable

convolutions and grouped convolutions, respectively. More sophisticated efficiency-enhancing grouping/sharing techniques are studied in [4].

Another strategy to accelerate CNNs is to exploit the low-rank structure prevalent in weight matrices and convolution kernels. [5, 6, 7] use tensor decompositions to obtain low-rank approximations of pretrained weight matrices/filter tensors and finetune the approximated weight matrices/filters to restore the accuracy of the compressed models. Other works [8, 9] employ low-rank promoting regularizers to further reduce the rank of the filter tensors. A framework to exploit low-rank structure in the filter responses is presented in [10].

Sparsifying filters and/or pruning channels are popular methods to make neural networks more efficient at inference. Works [11] and [12] rely on group norm-based regularizers and demonstrate their effectiveness in penalizing unimportant filters and channels, promoting hardware friendly filter shapes, regularizing the network depth, and optimizing the filter receptive fields. Inter-channel and intra-channel redundancy is exploited by [13] via a two-stage factorization procedure. An energy-aware methodology to prune filters of CNNs is described in [14].

Finally, an effective way to adapt DNNs to resource-constrained platforms is to reduce the numerical precision of their weights and/or activations. Examples for DNNs that quantize both weights and activations are DoReFa-Net [16] and XNOR-Net [17]. Other works use binary weights [15, 17] and ternary weights [18, 19] but maintain full precision values for the activations. Keeping the activations in full precision instead of quantizing them as well leads to a smaller decrease in computational cost, but can yield higher accuracy.

### 3 Learning fast matrix multiplications via SPNs

#### 3.1 Casting matrix multiplication as SPN

Given square matrices  $A, B \in \mathbb{R}^{n \times n}$ , the product  $C = AB$  can be represented as a 2-layer SPN

$$\text{vec}(C) = W_c[(W_b \text{vec}(B)) \odot (W_a \text{vec}(A))] \quad (1)$$

where  $W_a, W_b \in \mathbb{K}^{r \times n^2}$  and  $W_c \in \mathbb{K}^{n^2 \times r}$ ,  $\mathbb{K} := \{-1, 0, 1\}$  are fixed, and  $\odot$  denotes the element-wise product. The SPN (1) disentangles additions (and subtractions), encoded in the matrices  $W_a$ ,  $W_b$ , and  $W_c$ , and multiplications, realized exclusively by the operation  $\odot$  (see Fig. 1). The width of the hidden layer of the SPN,  $r$ , hence determines the number of multiplications used for the matrix multiplication; a naïve implementation of the matrix multiplication  $AB$  requires  $r = n^3$ . For  $n = 2$ ,<sup>1</sup> Strassen's matrix multiplication algorithm [20] specifies the following set of weights that satisfy (1) for  $r = 7$  (instead of  $r = 8$ )

$$W_a = \begin{pmatrix} 1 & 0 & 0 & 1 \\ 0 & 1 & 0 & 1 \\ 1 & 0 & 0 & 0 \\ 0 & 0 & 0 & 1 \\ 1 & 0 & 1 & 0 \\ -1 & 1 & 0 & 0 \\ 0 & 0 & 1 & -1 \end{pmatrix}, \quad W_b = \begin{pmatrix} 1 & 0 & 0 & 1 \\ 1 & 0 & 0 & 0 \\ 0 & 0 & 1 & -1 \\ -1 & 1 & 0 & 0 \\ 0 & 0 & 0 & 1 \\ 1 & 0 & 1 & 0 \\ 0 & 1 & 0 & 1 \end{pmatrix}, \quad W_c = \begin{pmatrix} 1 & 0 & 0 & 1 & -1 & 0 & 1 \\ 0 & 1 & 0 & 1 & 0 & 0 & 0 \\ 0 & 0 & 1 & 0 & 1 & 0 & 0 \\ 1 & -1 & 1 & 0 & 0 & 1 & 0 \end{pmatrix}. \quad (2)$$

An interesting tensor perspective on the SPN (1) (not explored in-depth here) is common in the context of algebraic complexity theory. Specifically, (1) can be written as

$$\text{vec}(C)_i = \sum_{k=1}^{n^2} \sum_{l=1}^{n^2} (M_n)_{i,k,l} \text{vec}(A)_k \text{vec}(B)_l, \quad \text{where} \quad (M_n)_{i,k,l} = \sum_{j=1}^r (W_c)_{i,j} (W_a)_{j,k} (W_b)_{j,l}.$$

<sup>1</sup>The formulation in [20] is more general, applying recursively to 4 equally-sized subblocks of square matrices, with the  $2 \times 2$  case occurring at maximal recursion depth.

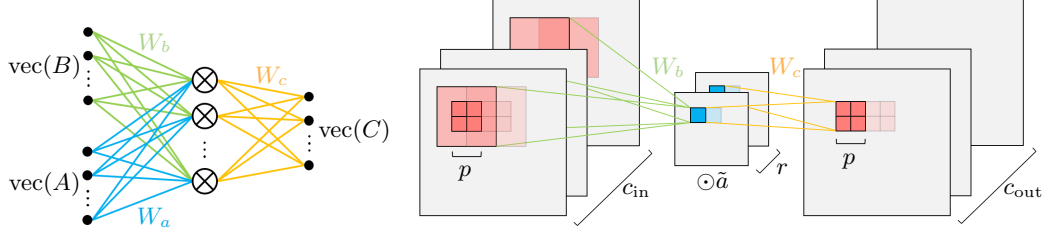


Figure 1: **Left:** Illustration of the SPN (1). The edges have weights in  $\mathbb{K} = \{-1, 0, 1\}$ . **Right:** Application of the proposed framework to 2D convolution leads to  $p$ -strided 2D convolution with  $W_b$ , followed by channel-wise scaling with by  $\tilde{a} = W_a \text{vec}(A)$ , followed by  $1/p$ -strided transposed 2D convolution with  $W_c$ .

$M_n$  is the  $(n \times n)$ -matrix multiplication tensor, and  $r$  hence corresponds to the rank of  $M_n$ . It is known that  $\text{rank}(M_2) = 7$  and  $19 \leq \text{rank}(M_3) \leq 23$ , see [26] for more details and references.

Elser [26] explores learning networks of the form (1) for  $n = 2$  and  $n = 3$  from data, relaxing the elements of  $W_a$ ,  $W_b$ , and  $W_c$  to be real numbers instead of elements from  $\mathbb{K}$ . It is observed in [26] that a learning rule termed *conservative learning* converges linearly for  $r = 7$  and  $n = 2$  in all simulation runs, and for  $r = 23$  and  $n = 3$  in 64% of the simulation runs.

### 3.2 Learning fast approximate matrix multiplications for DNNs

Writing matrix products in the form (1) is not specific to square matrices. Indeed, it is easy to see that the product of any two matrices  $A \in \mathbb{R}^{k \times m}$  and  $B \in \mathbb{R}^{m \times n}$ , including matrix-vector products (i.e.,  $n = 1$ ), can be written in the form (1) if  $r \geq nmk$ . When the matrices  $A$  and  $B$  are drawn from probability distributions that concentrate on low-dimensional manifolds of  $\mathbb{R}^{k \times m}$  and  $\mathbb{R}^{m \times n}$ , respectively, or if one of the matrices is fixed, it may be possible to find  $W_a$  and  $W_b$  that satisfy the equality in (1) (approximately) even when  $r \ll nmk$ . In this case, (1) (approximately) computes the product  $AB$  while considerably reducing the number of multiplications compared to the naïve implementation. Furthermore, by encoding structure (such as, e.g., sparsity or block-diagonal structure) into the matrices  $W_a$ ,  $W_b$ ,  $W_c$  one can tailor sharing or grouping of the operations for the application or platform at hand.

In this paper, we leverage this concept to accelerate and compress the matrix multiplications in DNN layers for inference. Specifically, for layer  $\ell$ , we associate  $A$  with the (pretrained) weights/filters  $W_\ell$  and  $B$  with the corresponding activations/feature maps  $F_\ell$ . The ternary matrices  $W_a$ ,  $W_b$ , and  $W_c$  are then learned end-to-end using a stochastic gradient-based optimizer (one set of weights  $W_a$ ,  $W_b$ ,  $W_c$  for each layer). After training,  $W_a$  and  $\text{vec}(A)$  can be collapsed into a vector  $\tilde{a} = W_a \text{vec}(A) \in \mathbb{R}^r$  as they are both fixed. Alternatively,  $\tilde{a} \in \mathbb{R}^r$ ,  $W_b$ , and  $W_c$  can be learned jointly from scratch. The choice of  $r$  determines the tradeoff between the computational cost in terms of multiplications and the precision of the the approximate matrix multiplication, and hence the accuracy of the network. Our approach requires  $r$  full-precision parameters and  $rm(k+n)$  ternary parameters, and reduces the number of multiplications by a factor of  $mnk/r$ .

Quantizing the elements of  $W_a$ ,  $W_b$ , and  $W_c$  to  $\mathbb{K}$  during training poses a challenge as quantization is non-differentiable. Different approaches were proposed to overcome this issue [15, 18, 17, 19, 27]. Here, we adopt the method from [18] and briefly describe it for quantizing  $W_a$  ( $W_b$  and  $W_c$  are quantized in exactly the same way). Specifically, this method maintains a full-precision version  $W_a^{\text{fp}}$  of  $W_a$  during training and quantizes it in every forward pass by approximately solving the optimization problem

$$\alpha^*, W_a^{\text{t}*} = \arg \min_{\alpha, W_a^{\text{t}}} \|W_a^{\text{fp}} - \alpha W_a^{\text{t}}\|_F^2 \quad \text{s.t.} \quad \alpha > 0, W_a^{\text{t}} \in \mathbb{K}^{r \times km} \quad (3)$$

and by setting  $W_a = \alpha^* W_a^{t*}$  (the scaling factors  $\alpha$  for  $W_a$ ,  $W_b$ ,  $W_c$  can be absorbed by  $A$  or  $\tilde{a}$  after training to ensure that  $W_a$ ,  $W_b$ ,  $W_c$  have elements in  $\mathbb{K}$ ). During the backward pass the quantization function is replaced by the identity function, and the gradient step is applied to the full precision version  $W_a^{\text{fp}}$  of  $W_a$ . Assuming i.i.d. Gaussian weights, [18] derives the approximate solution

$$(W_a^{t*})_{i,j} = \begin{cases} 1 & \text{if } (W_a^{\text{fp}})_{i,j} > \Delta, \\ -1 & \text{if } (W_a^{\text{fp}})_{i,j} < -\Delta, \\ 0 & \text{otherwise,} \end{cases} \quad \alpha^* = \frac{\sum_{(i,j): (W_a^{t*})_{i,j} \neq 0} |(W_a^{\text{fp}})_{i,j}|}{\sum_{i,j} |(W_a^{t*})_{i,j}|} \quad (4)$$

to (3), where  $\Delta = \frac{0.7}{k m r} \sum_{i,j} |(W_a^{\text{fp}})_{i,j}|$ . While our framework would allow quantized training from scratch with fixed threshold  $\Delta$  and quantization level  $\alpha$  (e.g.,  $\Delta = 0.5$  and  $\alpha = 1$ ), we observed that relying on the scheme (4) allows us to pretrain  $W_a^{\text{fp}}$ ,  $W_b^{\text{fp}}$ ,  $W_c^{\text{fp}}$  without quantization, and then activate quantization and stably continue training. We found that this strategy leads to faster training while inducing no loss in accuracy.

Besides the fully connected case described in this section, we particularize the proposed approach for 2D convolutions for image classification networks. We emphasize that any linear operation commonly performed in DNN layers can be cast into the form (1), including  $n$ -dimensional convolutions, group (equivariant) convolutions (when implemented as a filter bank) [28], and deformable convolutions [29].

### 3.3 Application to 2D convolution

Consider the  $\ell$ th 2D convolution layer of a CNN applying  $c_{\text{out}}$  filters of dimension  $w \times h \times c_{\text{in}}$  to a feature representation  $F$  of dimension  $W \times H \times c_{\text{in}}$  (width  $\times$  height  $\times$  number of channels). To write the computation of all  $c_{\text{out}}$  output channels as a matrix multiplication, each feature map in  $F$  is decomposed into  $WH$  patches of size  $w \times h$  (after appropriate padding) and the vectorized patches are arranged in a matrix  $\tilde{F}$  of dimension  $whc_{\text{in}} \times WH$  (this transformation is usually referred to as `im2col`, see [24, Fig. 19] for an illustration). Accordingly, the filters for all output channels are vectorized and jointly reshaped into a  $c_{\text{out}} \times whc_{\text{in}}$  matrix  $\tilde{W}_\ell$ . The vectorized layer output (before activation) for all  $c_{\text{out}}$  output channels is obtained as  $\tilde{W}_\ell \tilde{F}$  and has dimension  $c_{\text{out}} \times WH$ . In principle, one can now compress the operation  $\tilde{W}_\ell \tilde{F}$  using our method by setting  $A = \tilde{W}_\ell$ ,  $B = \tilde{F}$ , plugging them into (1), and proceeding as described in Section 3.2. However, this results in impractically large  $W_a$ ,  $W_b$ , and  $W_c$  and ignores the weight sharing structure of the convolution. By associating  $A$  with  $\tilde{W}_\ell$  and  $B$  with single columns of  $\tilde{F}$  we can jointly compress the filters across all input and output channels, while preserving the spatial structure of the convolution. The resulting operation can be thought of as a convolution with  $r$  ternary  $w \times h \times c_{\text{in}}$  filters (the rows of  $W_b$ ), followed by a channel-wise scaling with  $\tilde{a} = W_a \text{vec}(\tilde{W})$ , followed by convolution with a ternary  $1 \times 1$  filter for each of the  $c_{\text{out}}$  outputs (the rows of  $W_c$ , see Fig. 1).

To realize *local spatial compression*, we partition the computation of the convolution into subsets corresponding to square output patches. In more detail, we consider the computation of  $p \times p$  convolution output patches from  $(p-1+w) \times (p-1+h)$  input patches, offset by a stride of  $p$ , and approximate this computation with a SPN jointly for all channels. As a result, the number of multiplications is reduced both spatially and across channels. For example, for  $3 \times 3$  convolutional filters, we divide the input feature maps into  $4 \times 4$  spatial patches with a stride of 2, such that the SPN computes  $2 \times 2 \times c_{\text{out}}$  outputs from  $4 \times 4 \times c_{\text{in}}$  elements of  $F$ . Thereby,  $W_c$  realizes a  $2 \times 2 \times r$  transposed convolution with a stride of 1/2 (see Fig. 1). For fixed  $r$ , this reduces the number of multiplications by a factor 4 compared to the case without spatial compression (i.e.,  $p = 1$ ).

In summary, the described compression of 2D convolution leads to a reduction of the number of multiplications by a factor  $c_{\text{in}} c_{\text{out}} w h p^2 / r$  compared to the standard implementation of the convolution.

Finally, to reduce the number of additions by a factor of  $g$  (and thereby the number of nonzero elements of  $W_b$ ) we implement  $W_b$  as grouped convolution, originally introduced in [30]. Specifically, the convolution realized by  $W_b$  is assumed to consist of  $g$  independent 2D convolutions each with  $c_{\text{in}}/g$  input channels and  $r/g$  output channels, i.e.,  $W_b$  is assumed to be block-diagonal with blocks of dimension  $(r/g) \times (whc_{\text{in}}/g)$ .

**Relation to prior work in the 2D convolution case.** Binary weight networks (BWNs) [17] and ternary weight networks (TWNs) [18] rely on binary and ternary weight matrices, respectively, followed by (full-precision) rescaling of the activations (see Section 3.2) and are special cases of our approach. However, we do not directly recover the trained ternary quantization (TTQ) approach from [18], which relies on asymmetric ternary weights  $\{-c_1, 0, c_2\}$ ,  $c_1, c_2 > 0$ . Finally, note that Winograd filter-based convolution [21] realizes spatial compression over  $2 \times 2$  output patches but performs exact computation and does not compress across channels.

## 4 Experiments

### 4.1 Rediscovering Strassen’s algorithm

Before applying the proposed method to DNNs, we demonstrate that it is able to rediscover Strassen’s algorithm, i.e., it can learn to multiply  $2 \times 2$  matrices using only 7 multiplications instead of 8 (which implies a recursive algorithm for larger matrices). In contrast to prior work [26], which learns *real-valued* weight matrices  $W_a$ ,  $W_b$ ,  $W_c$  and increases the number of multiplications in general when using these matrices in (1) to compute matrix products, our method learns  $W_a, W_b \in \mathbb{K}^{7 \times 4}$ ,  $W_c \in \mathbb{K}^{4 \times 7}$  (i.e., the discrete solution space has size  $3^{3 \cdot 4 \cdot 7} = 3^{84}$ ), and hence leads to an actual reduction in the number of multiplications.

We generate a training set containing 100k pairs  $(A_i, B_i)$  with entries i.i.d. uniform on  $[-1, 1]$ , train the SPN with full precision weights (initialized i.i.d. uniform on  $[-1, 1]$ ) for one epoch with SGD (learning rate 0.1, momentum 0.9, mini-batch size 4), activate quantization, and train for another epoch (with learning rate 0.001). Around 25 random initializations are necessary to obtain convergence to zero training L2-loss after activation of the quantization; for most initializations the training L2-loss converges to a positive value. A set of ternary weight matrices found by our method is

$$W_a = \begin{pmatrix} -1 & -1 & 0 & 0 \\ 0 & 0 & 0 & 1 \\ -1 & -1 & 1 & 1 \\ -1 & 0 & 1 & 0 \\ -1 & -1 & 1 & 0 \\ 0 & 0 & 1 & 0 \\ 0 & -1 & 0 & 0 \end{pmatrix}, \quad W_b = \begin{pmatrix} -1 & -1 & 0 & 0 \\ 0 & 0 & 0 & 1 \\ 0 & 1 & 0 & 0 \\ 1 & 0 & 1 & 0 \\ -1 & -1 & -1 & 0 \\ 1 & 1 & 1 & 1 \\ 0 & 0 & -1 & 0 \end{pmatrix}, \quad W_c = \begin{pmatrix} 1 & 0 & 0 & -1 & -1 & 0 & 1 \\ 0 & 0 & 1 & 1 & 1 & 0 & -1 \\ -1 & 0 & 0 & 0 & 1 & 1 & -1 \\ 0 & 1 & 0 & 0 & 0 & 0 & 1 \end{pmatrix}.$$

Employing the same procedure (without hyperparameter tuning) to learn an algorithm for computing the product of two  $3 \times 3$  matrices with 23 multiplications did not lead to zero training L2-loss for any initialization we tried (a set of ternary  $W_a$ ,  $W_b$ ,  $W_c$  matrices is known for  $n = 3$  and  $r = 23$  from [31]).

### 4.2 Image classification

We applied our method to all convolutional layers (including the first convolutional layer and the projection layers for subsampling) of ResNet [32], evaluated the so-obtained Strassen-ResNet (ST-ResNet) on CIFAR-10 (10 classes, 50k training images, 10k testing images) and ImageNet (ILSVRC2012; 1k classes, 1.2M training images, 50k testing images) for different choices of  $r$ ,  $p$ ,  $g$ , and compare the accuracy of ST-ResNet to related works. All models

were trained from scratch, i.e., we directly learn  $\tilde{a} = W_a \text{vec}(A)$  rather than associating  $A$  with the weights of pretrained networks and learning  $W_a$ . Throughout, we used SGD with momentum 0.9 and weight decay  $10^{-4}$  for optimization. To facilitate comparisons, for all methods involving ternary weights we do not assume the weights to be sparse. It is the sparsity of the activations, not that of the weights, that directly impacts the number of multiplications. Assuming the same sparsity level for the activations and weights of all methods (excluding the weights of BNs [17]), all comparisons below remain valid. All model sizes are computed without (lossless) compression.

#### 4.2.1 CIFAR-10<sup>2</sup>

We consider ST-ResNet-20 and first learn full-precision values for  $\tilde{a}$ ,  $W_b$ , and  $W_c$ , employing the data augmentation procedure described in [32, Sec. 4.2.]. We train for 250 epochs with initial learning rate 0.1, multiplying the learning rate by 0.1 after 150 and 200 epochs. We then activate quantization for  $W_b$  and  $W_c$ , set the learning rate to 0.01 and train the network for 40 epochs, multiplying the learning rate by 0.1 every 10 epochs. Finally, we fix the (now ternary)  $W_b$  and  $W_c$  and continue training for another 10 epochs. The resulting testing accuracy is shown in Table 1 for different  $r$  and different  $p$ , along with the total reduction in computational cost compared to the uncompressed model in Table 2 (for the  $32 \times 32$  CIFAR-10 images).

**Discussion.** The model obtained for the base configuration with  $r = c_{\text{out}}$  and  $p = 1$  incurs a negligible accuracy loss compared to the uncompressed ResNet-20 with an accuracy of 91.25% while reducing the number of multiplications by 98.96% (the evaluation of the uncompressed ResNet-20 requires 41.038M multiply-adds). This model also matches the accuracy of TTQ [19] for ResNet-20 while requiring fewer multiplications than TTQ (as TTQ does not quantize the first convolutional layer). As  $r$  decreases and/or  $p$  increases, the number of multiplications decreases at the cost of further accuracy reduction.

$p$	$c_{\text{out}}$	$r$		
		$\frac{3}{4}c_{\text{out}}$	$\frac{1}{2}c_{\text{out}}$	$\frac{1}{4}c_{\text{out}}$
1	91.24	90.62	88.63	85.46
2	89.87	89.47	87.31	84.01
4	86.13	84.67	82.67	75.01

Table 1: Testing accuracy (in %) of compressed ResNet-20 on CIFAR-10

multiplications					additions				
$p$	$c_{\text{out}}$	$r$			$p$	$c_{\text{out}}$	$r$		
		$\frac{3}{4}c_{\text{out}}$	$\frac{1}{2}c_{\text{out}}$	$\frac{1}{4}c_{\text{out}}$			$\frac{3}{4}c_{\text{out}}$	$\frac{1}{2}c_{\text{out}}$	$\frac{1}{4}c_{\text{out}}$
1	98.962	99.084	99.207	99.329	1	-13.904	14.435	42.774	71.112
2	99.329	99.359	99.390	99.420	2	39.123	54.205	69.287	84.369
4	99.420	99.428	99.436	99.443	4	57.550	68.025	78.501	88.976

Table 2: Reduction (in %) in the number of operations obtained by our method for ResNet-20.

<sup>2</sup>Code available at <https://github.com/mitscha/strassennets>.

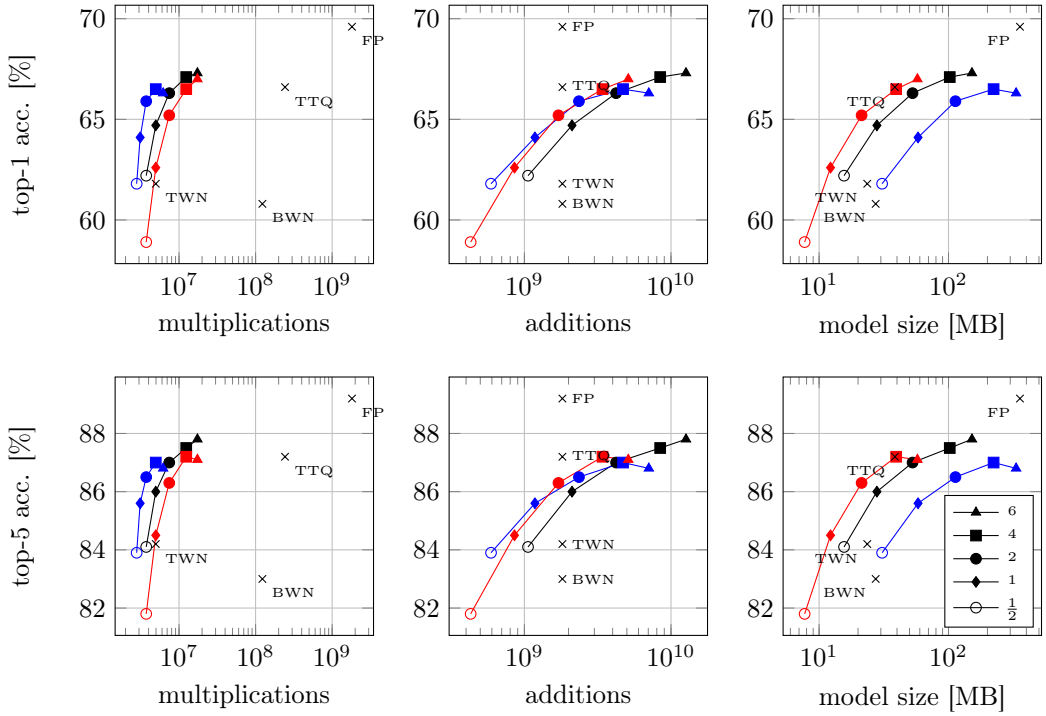


Figure 2: Top-1 and top-5 validation accuracy of ST-ResNet-18 on ImageNet as a function of total number of multiplications, the number of additions, and model size, along with the values obtained in related works BWN [17], TWN [18], TTQ [19], and the full precision model (FP). The numbers associated with the mark types correspond to the ratio of the number of hidden SP units and output channels,  $r/c_{\text{out}}$ . Different colors indicate different combinations of output patch size  $p$  and number of convolution groups  $g$ : Blue:  $p = 2, g = 1$ ; black:  $p = 1, g = 1$ ; red:  $p = 1, g = 4$ .

#### 4.2.2 ImageNet

We consider ST-ResNet-18 and, again, we first learn full-precision values for  $\tilde{a}$ ,  $W_b$ , and  $W_c$ . Unlike for the experiment on CIFAR-10 (which has only 10 classes and hence a small fully-connected layer), we also compress the last (fully connected) layer of ST-ResNet-18, setting  $r = 1000$  for that layer throughout. Following [17, 18, 19], the training images are resized such that the shorter side has length 256 and are then randomly cropped to  $224 \times 224$  pixels. The validation accuracy is computed from center crops. We use an initial learning rate of 0.1, with two different learning rate schedules depending on the value of  $r$  in the compressed convolutional layers: We train for 40 epochs without quantization, multiplying the learning rate by 0.1 after 30 epochs, if  $r/c_{\text{out}} \leq 1$ , and for 70 epochs, multiplying the learning rate by 0.1 after 40 and 60 epochs, otherwise. Thereafter, we activate quantization and continue training for 10 epochs. Finally, we fix  $W_b$  and  $W_c$  and continue training  $\tilde{a}$  for 5 epochs.

Table 3 shows the accuracy of ST-ResNet-18 for different  $r$ ,  $p$ , and  $g$ . In Table 5 we report the reduction in the number of operations and model size compared to the original ResNet-18 model, for different  $r$ ,  $p$ , and  $g$ . The accuracy of related methods [17, 18, 19] and the original ResNet-18 model, along with the corresponding reduction in the number of operations and model size is shown in Table 4. In Figure 2, we plot the accuracy of ST-ResNet-18 for different  $r$ ,  $p$ , and  $g$ , as a function of the number of operations and model size.

**Discussion.** All ST-ResNet-18 models that require the same number of multiplications as TWN (i.e., those with  $r = c_{\text{out}}$ ,  $p = 1$ , and  $g = 4$ ;  $r = c_{\text{out}}$ ,  $p = 1$ , and  $g = 1$ ;  $r = 4c_{\text{out}}$ ,  $p = 2$ , and  $g = 1$ ) obtain a considerably higher top-1 and top-5 accuracy than TWN. In particular, ST-ResNet-18 with  $r = 4c_{\text{out}}$ ,  $p = 2$ , and  $g = 1$  leads to a 7.6% improvement in top-1 accuracy. Furthermore, ST-ResNet-18 with  $r = c_{\text{out}}$ ,  $p = 2$ , and  $g = 1$  matches the top-1 accuracy of TWN while using 43.7% fewer multiplications and 67.4% fewer additions. ST-ResNet-18 with  $r = 4c_{\text{out}}$ ,  $p = 1$ , and  $g = 1$  outperforms TTQ while using 94.9% fewer multiplications. The same ST-ResNet-18 model incurs a top-5 accuracy reduction of only 1.9% compared to the full precision model while reducing the number of multiplications by 99.3%. Note that TTQ and BWN use considerably more multiplications than ST-ResNet-18 and TWN as they do not quantize the first and the last layer.

For some of the configurations, the reduction in the number of multiplications comes at the cost of a small to moderate increase in the number of additions and model size. We emphasize that this is also the case for Strassen’s algorithm (see (2)) and the Winograd filter-based convolution (see [21, Sec. 4.1]). Moreover, it can be observed that increasing the ratio  $r/c_{\text{out}}$  from 4 to 6 only leads to a small increase in accuracy, or even to a reduction. A possible explanation for this behavior is that optimization the ternary weight matrices could become hard as the matrices become large due to the way they interact in the SPNs. Finally, in all our experiments the ratio  $r/c_{\text{out}}$  is the same for all layers, and one would expect improvements from allocating more multiplications to layers that require more accurate operations. A simple way to learn the ratio  $r/c_{\text{out}}$  for each layer from data is to choose  $r/c_{\text{out}}$  large and to apply L1 regularization to the vectors  $\tilde{a}$ . However, this strategy led to lower accuracy for a given multiplication budget in our experiments than just fixing  $r/c_{\text{out}}$  for all layers.

top-1 accuracy						top-5 accuracy								
		$r$								$r$				
$(p, g)$		$6c_{\text{out}}$	$4c_{\text{out}}$	$2c_{\text{out}}$	$c_{\text{out}}$	$\frac{1}{2}c_{\text{out}}$		$(p, g)$		$6c_{\text{out}}$	$4c_{\text{out}}$	$2c_{\text{out}}$	$c_{\text{out}}$	$\frac{1}{2}c_{\text{out}}$
(1, 1)		67.3	67.1	66.3	64.7	62.2		(1, 1)		87.8	87.5	87.0	86.0	84.1
(2, 1)		66.3	66.5	65.9	64.1	61.8		(2, 1)		86.8	87.0	86.5	85.6	83.9
(1, 4)		67.0	66.5	65.2	62.6	58.9		(1, 4)		87.1	87.2	86.3	84.5	81.8

Table 3: Top-1 and top-5 validation accuracy (in %) of ST-ResNet-18 on ImageNet, for different choices of  $r$ ,  $p$ , and  $g$ .

	top-1	top-5	multiplications	model size
BWN [17]	60.8	83.0	93.25	92.33
TWN [18]	61.8	84.2	99.73	93.39
TTQ [19]	66.6	87.2	86.66	89.20
ST ( $r = 4c_{\text{out}}$ , $p = 1$ , $g = 1$ )	67.1	87.5	99.32	71.33
full precision	69.6	89.2	$(1.82 \cdot 10^9)$	(356.74 MB)

Table 4: Top-1 and top-5 validation accuracy (in %) along with the reduction (in %) in the number of multiplications, and model size for ResNet-18, compared to the full precision model (for the full precision model, the absolute quantities are given in parentheses).

model size						
$(p, g)$		$r$				
		$6c_{\text{out}}$	$4c_{\text{out}}$	$2c_{\text{out}}$	$c_{\text{out}}$	$\frac{1}{2}c_{\text{out}}$
(1, 1)		57.45	71.33	85.22	92.16	95.63
(2, 1)		6.64	37.46	68.28	83.69	91.4
(1, 4)		83.88	88.95	94.03	96.56	97.83

multiplications						additions						
$(p, g)$		$r$					$r$					
		$6c_{\text{out}}$	$4c_{\text{out}}$	$2c_{\text{out}}$	$c_{\text{out}}$	$\frac{1}{2}c_{\text{out}}$	$(p, g)$	$6c_{\text{out}}$	$4c_{\text{out}}$	$2c_{\text{out}}$	$c_{\text{out}}$	$\frac{1}{2}c_{\text{out}}$
(1, 1)		99.04	99.32	99.59	99.73	99.79	(1, 1)	-596.81	-364.61	-132.42	-16.32	41.73
(2, 1)		99.66	99.73	99.79	99.83	99.85	(2, 1)	-288.62	-159.15	-29.69	35.05	67.41
(1, 4)		99.04	99.32	99.59	99.73	99.79	(1, 4)	-181.56	-87.78	6.00	52.89	76.33

Table 5: Reduction in the number of multiplications, additions, and model size (in %) of ST-ResNet-18 compared to the full-precision model, for different choices of  $r$ ,  $p$ , and  $g$ .

## 5 Conclusion and future work

We proposed and evaluated a versatile framework to learn fast approximate matrix multiplications for DNNs end-to-end. We found that our method yields significantly higher accuracy than existing methods for a given multiplication budget, or leads to the same or higher accuracy compared to existing methods while using significantly fewer multiplications. In future work, we plan to explore knowledge transfer from pretrained models to further improve the accuracy of our compressed models. Moreover, it will be interesting to see how the theoretical gains reported here translate into runtime speedups on specialized hardware such as FPGAs.

**Acknowledgment:** We would like to thank Eirikur Agustson, Helmut Bölcskei, Lukas Cavigelli, Risi Kondor, Zachary C. Lipton, Weitang Liu, John Owens, Sheng Zha, and Zhi Zhang for inspiring discussions and comments.

## References

- [1] F. N. Iandola, S. Han, M. W. Moskewicz, K. Ashraf, W. J. Dally, and K. Keutzer, “SqueezeNet: AlexNet-level accuracy with 50x fewer parameters and < 0.5 MB model size,” *arXiv:1602.07360*, 2016.
- [2] A. G. Howard, M. Zhu, B. Chen, D. Kalenichenko, W. Wang, T. Weyand, M. Andreetto, and H. Adam, “Mobilenets: Efficient convolutional neural networks for mobile vision applications,” *arXiv:1704.04861*, 2017.
- [3] X. Zhang, X. Zhou, M. Lin, and J. Sun, “Shufflenet: An extremely efficient convolutional neural network for mobile devices,” *arXiv:1707.01083*, 2017.
- [4] M. Wang, B. Liu, and H. Foroosh, “Design of efficient convolutional layers using single intra-channel convolution, topological subdivisioning and spatial “bottleneck” structure,” *arXiv:1608.04337*, 2016.
- [5] E. L. Denton, W. Zaremba, J. Bruna, Y. LeCun, and R. Fergus, “Exploiting linear structure within convolutional networks for efficient evaluation,” in *Advances in Neural Information Processing Systems*, 2014, pp. 1269–1277.

- [6] A. Novikov, D. Podoprikin, A. Osokin, and D. P. Vetrov, “Tensorizing neural networks,” in *Advances in Neural Information Processing Systems*, 2015, pp. 442–450.
- [7] Y.-D. Kim, E. Park, S. Yoo, T. Choi, L. Yang, and D. Shin, “Compression of deep convolutional neural networks for fast and low power mobile applications,” in *Int. Conf. on Learning Representations*, 2016.
- [8] C. Tai, T. Xiao, Y. Zhang, X. Wang *et al.*, “Convolutional neural networks with low-rank regularization,” *arXiv:1511.06067*, 2015.
- [9] W. Wen, C. Xu, C. Wu, Y. Wang, Y. Chen, and H. Li, “Coordinating filters for faster deep neural networks,” *arXiv:1703.09746*, 2017.
- [10] X. Zhang, J. Zou, K. He, and J. Sun, “Accelerating very deep convolutional networks for classification and detection,” *IEEE Trans. on Pattern Analysis and Machine Intelligence*, vol. 38, no. 10, pp. 1943–1955, 2016.
- [11] W. Wen, C. Wu, Y. Wang, Y. Chen, and H. Li, “Learning structured sparsity in deep neural networks,” in *Advances in Neural Information Processing Systems*, 2016, pp. 2074–2082.
- [12] V. Lebedev and V. Lempitsky, “Fast convnets using group-wise brain damage,” in *Proc. IEEE Conf. on Computer Vision and Pattern Recognition*, 2016, pp. 2554–2564.
- [13] B. Liu, M. Wang, H. Foroosh, M. Tappen, and M. Pensky, “Sparse convolutional neural networks,” in *Proc. IEEE Conf. on Computer Vision and Pattern Recognition*, 2015, pp. 806–814.
- [14] T.-J. Yang, Y.-H. Chen, and V. Sze, “Designing energy-efficient convolutional neural networks using energy-aware pruning,” *arXiv:1611.05128*, 2016.
- [15] M. Courbariaux, Y. Bengio, and J.-P. David, “Binaryconnect: Training deep neural networks with binary weights during propagations,” in *Advances in Neural Information Processing Systems*, 2015, pp. 3123–3131.
- [16] S. Zhou, Y. Wu, Z. Ni, X. Zhou, H. Wen, and Y. Zou, “DoReFa-Net: Training low bitwidth convolutional neural networks with low bitwidth gradients,” *arXiv:1606.06160*, 2016.
- [17] M. Rastegari, V. Ordonez, J. Redmon, and A. Farhadi, “XNOR-Net: Imagenet classification using binary convolutional neural networks,” in *European Conf. on Computer Vision*. Springer, 2016, pp. 525–542.
- [18] F. Li, B. Zhang, and B. Liu, “Ternary weight networks,” *arXiv:1605.04711*, 2016.
- [19] C. Zhu, S. Han, H. Mao, and W. J. Dally, “Trained ternary quantization,” *arXiv:1612.01064*, 2016.
- [20] V. Strassen, “Gaussian elimination is not optimal,” *Numerische Mathematik*, vol. 13, no. 4, pp. 354–356, 1969.
- [21] A. Lavin and S. Gray, “Fast algorithms for convolutional neural networks,” in *Proc. IEEE Conf. on Computer Vision and Pattern Recognition*, 2016, pp. 4013–4021.
- [22] M. Horowitz, “Computing’s energy problem (and what we can do about it),” in *IEEE Int. Solid-State Circuits Conf. Digest of Technical Papers*, 2014, pp. 10–14.
- [23] R. Andri, L. Cavigelli, D. Rossi, and L. Benini, “Yodann: An architecture for ultra-low power binary-weight cnn acceleration,” *IEEE Trans. on Computer-Aided Design of Integrated Circuits and Systems*, 2017.

- [24] V. Sze, Y.-H. Chen, T.-J. Yang, and J. Emer, “Efficient processing of deep neural networks: A tutorial and survey,” *arXiv:1703.09039*, 2017.
- [25] E. Nurvitadhi, G. Venkatesh, J. Sim, D. Marr, R. Huang, J. O. G. Hock, Y. T. Liew, K. Srivatsan, D. Moss, S. Subhaschandra, and G. Boudoukh, “Can FPGAs beat GPUs in accelerating next-generation deep neural networks?” in *FPGA*, 2017, pp. 5–14.
- [26] V. Elser, “A network that learns strassen multiplication,” *Journal of Machine Learning Research*, vol. 17, no. 116, pp. 1–13, 2016.
- [27] E. Agustsson, F. Mentzer, M. Tschannen, L. Cavigelli, R. Timofte, L. Benini, and L. Van Gool, “Soft-to-hard vector quantization for end-to-end learned compression of images and neural networks,” *arXiv:1704.00648*, 2017.
- [28] T. Cohen and M. Welling, “Group equivariant convolutional networks,” in *Int. Conf. on Machine Learning*, 2016, pp. 2990–2999.
- [29] J. Dai, H. Qi, Y. Xiong, Y. Li, G. Zhang, H. Hu, and Y. Wei, “Deformable convolutional networks,” *arXiv:1703.06211*, 2017.
- [30] A. Krizhevsky, I. Sutskever, and G. E. Hinton, “Imagenet classification with deep convolutional neural networks,” in *Advances in Neural Information Processing Systems*, 2012, pp. 1097–1105.
- [31] J. D. Laderman, “A noncommutative algorithm for multiplying  $3 \times 3$  matrices using 23 multiplications,” *Bulletin of the American Mathematical Society*, vol. 82, no. 1, pp. 126–128, 1976.
- [32] K. He, X. Zhang, S. Ren, and J. Sun, “Deep residual learning for image recognition,” in *Proc. IEEE Conf. on Computer Vision and Pattern Recognition*, 2016, pp. 770–778.